



COPY RIGHT



2019IJIEMR. Personal use of this material is permitted. Permission from IJIEMR must be obtained for all other uses, in any current or future media, including reprinting/republishing this material for advertising or promotional purposes, creating new collective works, for resale or redistribution to servers or lists, or reuse of any copyrighted component of this work in other works. No Reprint should be done to this paper, all copy right is authenticated to Paper Authors

IJIEMR Transactions, online available on 4th Sept 2019. Link

[:http://www.ijiemr.org/downloads.php?vol=Volume-08&issue=ISSUE-09](http://www.ijiemr.org/downloads.php?vol=Volume-08&issue=ISSUE-09)

Title **3-STAGE SHUNT ACTIVE POWER FILTER**

Volume 08, Issue 09, Pages: 435–447.

Paper Authors

K SUMA,G SAI HARINI,G PHANITHA KRISHNA

Anu Bose Institute of Technology K.S.P Road, New paloncha, Bhadradi Kothagudem, Telangana, India



USE THIS BARCODE TO ACCESS YOUR ONLINE PAPER

To Secure Your Paper As Per **UGC Guidelines** We Are Providing A Electronic Bar Code

3-STAGE SHUNT ACTIVE POWER FILTER

K SUMA¹, G SAI HARINI², G PHANITHA KRISHNA³

^{1,2,3}UG Students, Dept. of Electrical and Electronics Engineering Anu Bose Institute of Technology
KSPRoad, Newpaloncha, Bhadradi Kothagudem, Telangana, India.
mallesham2070@gmail.com¹, g.harini002@gmail.com², gphanitha123@gmail.com³

Abstract:- Shunt dynamic power filters (SAPF) are utilized to improve control quality by infusing remunerating consonant current. The secluded SAPF offers numerous new abilities that are generally inaccessible by the ordinary SAPF, for example, high peak factor remunerating present and quick powerful reaction. In any case, there are still difficulties that should have been tended to, for example, reverberation and strength issues related with the particular SAPF. To research these issues, this work first shows a numerical model for customary measured SAPF framework. In light of the scientific investigation, another mixture three-level secluded SAPF is introduced that is made out of two kinds of modules, each with various current conveying limits, LCL channel parameters and exchanging frequencies. The proposed half and half framework gives a more extensive current following data transmission and quick unique reaction when contrasted with the present measured SAPF. An epic self-versatile, dynamic damping technique is suggested that successfully stifles reverberation and coupling between modules. Scientific examination and trial results have been utilized to check the proposed framework.

Index Terms:- SAPF, Modeling, Hybrid Modular, Three-level

I. INTRODUCTION

With an expansion in infiltration of nonlinear loads all through the power conveyance framework, current symphonious contamination at the matrix side is developing. The expanding number of higher request music causes a progression of issues, including voltage and current burdens, electro-attractive obstruction (EMI), and power transmission misfortunes [1], [2]. In like manner, inactive and dynamic symphonious relief procedures have been a noteworthy focal point of research as of late [3], [4]. Shunt Active Power Filters (SAPF) are used to alleviate sounds at the heap end by infusing a remunerating symphonious current

equivalent in extent and inverse in stage to that being drawn by nonlinear burdens connected [5]–[9]. Essentially, the SAPF carries on as a network tied inverter however supplies higher request music current with higher current peak factor and higher current slew rate [10]. The measured or parallel SAPF examined in an improvement over the customary SAPF. Given high peak factor and slow pace of the remunerating current it can deliver, the measured SAPF apparently gives the more compelling answer for symphonious contortion rather than the regular brought together SAPF structure. Improved performance can be watched particularly as far as following accuracy and

dynamic reaction, since the repaying current equitably disseminated between different modules. Notwithstanding, it will be later shown through numerical displaying in segment II, that it is hard for the regular structure of secluded or parallel SAPF to arrive an ideal harmony between quick unique reaction and stable control performance. The particular SAPF structure is fundamentally the same as that of parallel inverters. The coupling and reverberation between inverters are significant territories of research that have been very much tended to for parallel inverters [16]–[22]. Displaying of parallel inverters, hypothetical examination of reverberation and communications between parallel inverters has been talked about in. It is reasoned that the reverberation between inverters is enormously affected by yield channel inductance and lattice impedance. In this manner, expectedly, the reverberation is stifled by the LCL channel inductance guideline or structure plan as those in . Lately, dynamic damping has been widely explored to improve the change proficiency and current following accuracy. J. He, et al. have exhibited dynamic reverberation stifling systems by managing the control laws and applying framework the reverberation concealment and control soundness are the most significant issues with SAPF. Two basic reverberation concealment plans are recommended in the main technique diminishes dull control force at the expense of diminished remuneration exactness, while the subsequent strategy intends to reinforce inactive damping approach through expansion of a damping resistor at the expense of a higher power misfortune. Comparable issues have been tended to in for parallel SAPF which demonstrates that expanding the inductance and diminishing

the relative addition in PR controllers is compelling stifling reverberation conditions. The equipment basic highlights & dynamic reaction capacities of SAPF are not completely talked about in which secluded or parallel SAPFs have been basically treated as parallel sine wave inverters. The reverberation concealment strategies produced for SAPF are constrained to latent damping plans. In any case, it ought to be noticed that symphonious repaying current blunder following of SAPF contrasts eminently from the yield mistake following of customary sine wave inverters, particularly as far as solidness and dynamic reaction. The nearness of higher request music up to the 50th request in SAPF yield converts into a higher peak factor in current. Consequently, the SAPF requires quicker unique reaction and more noteworthy control data transfer capacity. Because of the previously mentioned issue the channel inductance for SAPF is typically intended to be substantially less than that of a regular sine wave inverter. The lower channel inductance represents a more serious danger of the reverberation condition between parallel SAPF modules while likewise lessening edge for reverberation concealment dynamic and inactive methods. Given their central contrasts from the progressively hard to touch base at a tradeoff between reverberation concealment and dynamic reaction capacity in secluded SAPF. In this manner, neither of the dynamic or inactive reverberation concealment strategies can be legitimately used from traditional inverters as indicated in. This paper presents abilities to address previously mentioned issues related with measured SAPF. Initial, an improved numerical model for a summed up three-level secluded SAPF that incorporates a present controller, framework impedance, and dynamic

damping plans is created. In view of the numerical investigation, we further propose a half breed three-level secluded SAPF framework that is made out of two sorts of modules with limits of 100A and 50A, individually. The 50A module has lower LCL channel parameters & higher changing recurrence to remunerate sounds of requests higher than thirteenth, and the 100A module has bigger LCL parameters and lower changing recurrence to address the music of lower request. Last, anovel self-versatile dynamic technique is proposed and actualized for the secluded SAPF to smother reverberation current between modules. The scientific examination and test outcomes exhibit that the proposed reverberation control system can improve the repaying data transfer capacity and solidness alongside quick and exact sounds following capacity.

II. MODELING OF THREE-LEVEL MODULAR SAPF

A. Modeling of a single three-level SAPF

SAPF is basically a controlled current source with yield current criticism control. Each SAPF module is associated with the network through a LCL channel as appeared in Fig.1. L_1 , L_2 , C , and L_g speak to SAPF side inductor, matrix side inductor, channel capacitor, and framework impedance, individually.

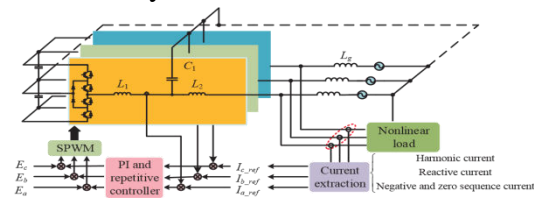


Fig. 1. General structure of three-level SAPF

The control plan of a solitary SAPF is appeared in Fig.2. Despite the fact that the reference current can be contributed by symphonious flows, responsive power, and

unbalance (negative and zero succession parts) in the heap, this paper essentially centers around consonant flows remuneration. Sounds are gotten by the specific symphonious identification calculation dependent on Discrete Fourier Transform (DFT). I_{ref} speaks to the reference current, $u_g(s)$ is the lattice voltage and $E(s)$ is the feed-forward estimation of $u_g(s)$. The criticism control of the present circle is acknowledged in A-B-C pivot by a redundant controller in parallel with a PI controller.

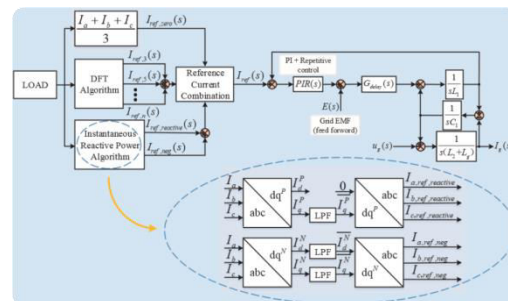


Fig. 2. Control diagram of modular SAPF
According to the control diagram in Fig.2, the transfer function of the output current to the reference current reads.

$$I_g(s) = \{PIR(s)G_{delay}(s)I_{ref}(s) - [s^2L_1C_1 + sC_1PIR(s)G_{delay}(s) - G_{delay}(s) + 1]E(s)\} / [s^2C_1(L_2 + L_g)PIR(s)G_{delay}(s) + s(L_1 + L_2 + L_g) - sL_gG_{delay}(s) + PIR(s)G_{delay}(s) + s^3L_1C_1(L_2 + L_g)] \quad (1)$$

where $I_g(s)$ speaks to yield current, $PIR(s)$ is the exchange capacity of the PI and the monotonous controller utilized, and G_{delay} speaks to the deferral because of framework examining, count and transmission [23]. Fig.3 demonstrates the disentangled, single three-level SAPF model proposed in this paper used to build the secluded framework. The impedance averaging model and little sign linearization methods have been utilized considering the distinction of SAPF from the sine wave inverter models as exhibited in [24], [25]. The proposed model can be isolated into two sections: the present source inverter and the lattice. The present source inverter is

made out of the reference current $I_{ref}(s)$, channel impedance $Z_F(s)$ and parallel yield impedance $Z_I(s)$ presented through input control. The lattice is portrayed by framework EMF $E(s)$, and matrix impedance $Z_g(s)$.

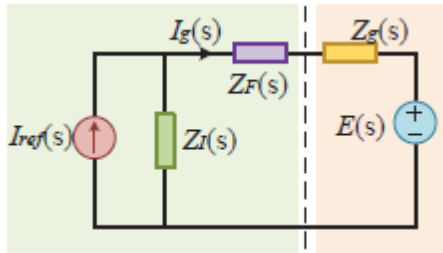


Fig. 3. The proposed single SAPF model in this paper

In light of the comparable model and the superposition hypothesis, the yield current $I_g(s)$ of a solitary SAPF can be composed.

$$I_g(s) = \frac{Z_I(s)I_{ref}(s) - E(s)}{Z_I(s) + Z_F(s) + Z_g(s)} \quad (2)$$

$Z_I(s)$ and $Z_F(s)$ can be gotten by illuminating Eqs (1) and (2)

$$Z_I(s) = \frac{PIR(s)G_{delay}(s)}{s^2L_1C_1 + sC_1PIR(s)G_{delay}(s) - G_{delay}(s) + 1} \quad (3)$$

$$Z_F(s) = \frac{s^3L_1C_1L_2 + s(L_1 + L_2) + s^2C_1L_2PIR(s)G_{delay}(s)}{s^2L_1C_1 + sC_1PIR(s)G_{delay}(s) - G_{delay}(s) + 1} \quad (4)$$

B. Modeling of parallel three-level SAPF system

In light of the model determined for a solitary three-level SAPF, the structure and model of the measured SAPF framework can be gotten as appeared in Fig.4. Each SAPF module has an autonomous controller, DC transport, and LCL yield channel. For instance, the exchange capacity of SAPF #1 can be gotten utilizing Kirchhoff's present law and the superposition hypothesis as appeared in Eq.(5).

$$I_{g-1}(s) = G_P(s)I_{ref,1}(s) + \sum_{n=2}^N G_N(s)I_{ref,n}(s) + G_E(s)E(s) \quad (5)$$

where N is the quantity of parallel units. There are three segments in Eq.(5) meaning

three animating sources from the particular framework, which are: current reference of SAPF #1 spoken to by $I_{ref} 1$, current references of other parallel SAPF spoken to by $I_{ref} n$, and matrix voltage speak to by $E(s)$. $G_P(s)$, $G_N(s)$ and $G_E(s)$ speak to move elements of these three invigorating sources to $I_g 1(s)$, separately.

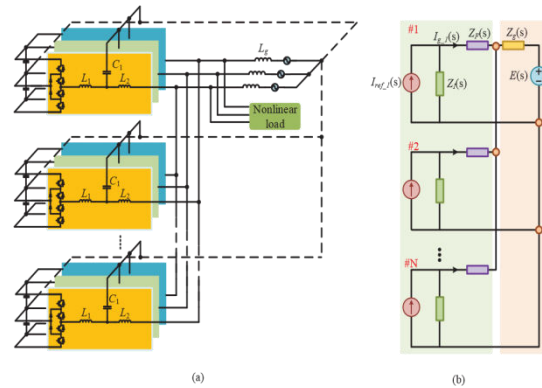


Fig. 4. Parallel structure of modular three-level SAPF

Fig.5 demonstrates the comparable circuits when SAPF 1# is energized by the three distinct sources referenced. As indicated by the superposition hypothesis, these three can be dealt with independently as appeared in Fig.5 (a), (b), and (c). Fig.5(a) is the proportionate circuit model energized by $I_{ref} 1$. The remaining $(N-1)$ SAPFs are treated as $(N-1)$ impedances in parallel: $Z_F(s)/(N-1)$ and $Z_I(s)/(N-1)$. Fig.5(b) demonstrates the proportionate circuit model energized by $E(s)$, wherein, all SAPF are viewed as impedances. Finally, Fig.5(c) demonstrates the equal model energized by $I_{ref} N$. The impedance of residual $(N-2)$ parallel inverters is $Z_F(s)/(N-2)$ and $Z_I(s)/(N-2)$.

From the proportionate circuits appeared in Fig.5, $G_P(s)$, $G_N(s)$ and $G_E(s)$ are inferred as following:

$$G_P(s) = \frac{Z_I(s)[Z_I(s) + Z_F(s) + (N-1)Z_g(s)]}{[Z_I(s) + Z_F(s)][Z_I(s) + Z_F(s) + NZ_g(s)]} \quad (6)$$

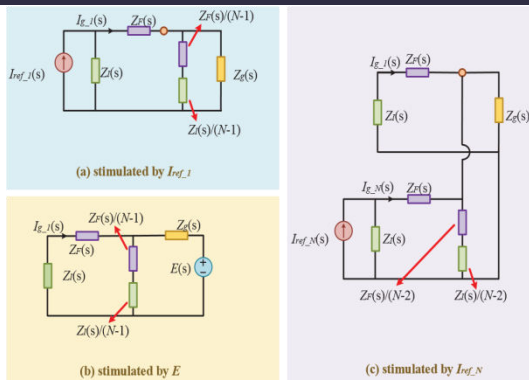


Fig. 5. SAPF #1 stimulated by three sources

$$G_N(s) = \frac{-Z_I(s)Z_g(s)}{[Z_I(s) + Z_F(s)][Z_I(s) + Z_F(s) + NZ_g(s)]} \quad (7)$$

$$G_E(s) = \frac{-1}{Z_I(s) + Z_F(s) + NZ_g(s)} \quad (8)$$

If each SAPF has the same output current, we obtain

$$I_{ref_1}(s) = I_{ref_2}(s) = \dots = I_{ref_n}(s) \quad (9)$$

$$I_{g_1}(s) = G_P(s)I_{ref_1}(s) + (N-1)G_N(s)I_{ref_n}(s) + G_E(s)E(s) = \frac{Z_I(s)I_{ref_1}(s) - E(s)}{Z_I(s) + Z_F(s) + NZ_g(s)} \quad (10)$$

Contrasting Eq.(10) against Eq.(2), it very well may be discovered that for a particular SAPF, for example, previously mentioned SAPF #1, the expansion in the quantity of SAPF associated in parallel makes the proportionate network impedance increment by N times. This can be affirmed promptly by the displaying circuit in Fig.6. Given same parameters for LCL channel and control calculation, the yield impedance $Z_F(s)$ of each SAPF module is the equivalent. Each SAPF module is associated at the purpose of basic coupling(PCC) with matrix impedance $Z_g(s)$. As appeared in Fig.6(b), $Z_g(s)$ can be treated as N divisions of $N \cdot Z_g(s)$ in parallel. Since yield current of each SAPF is the equivalent, PCC can be moved to one side as appeared in Fig.6(c). $Z_F(s)$ and $N \cdot Z_g(s)$ are then associated in arrangement as appeared in Fig.6(c). In this manner, it very well may be unmistakably demonstrated that the proportionate lattice

impedance of N parallel SAPF frameworks is expanded by N times. Given the exchange above it is express to comprehend that the full pinnacle of the exchange capacity of a SAPF module shifts towards left when the quantity of paralleled SAPF increments as appeared by the Bode plot in Fig.7. The stage plot in Fig.7 demonstrates that framework strength edge diminishes with expanded N, which represents a more prominent test to the control data transmission edge and reverberation concealment of ordinary measured SAPF. Unlike sine wave matrix tied inverters, SAPF infuses high recurrence consonant current running from 150Hz to 1500Hz as appeared by the concealed region in Fig.7, as opposed to the principal

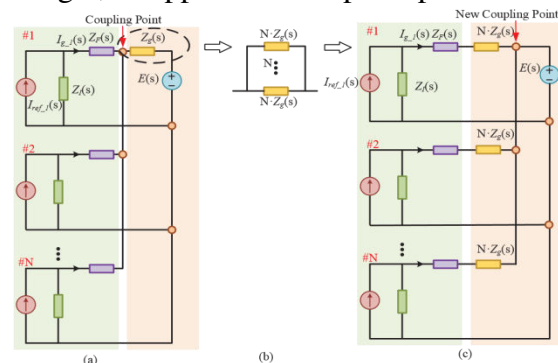


Fig. 6. Modeling of modular SAPF

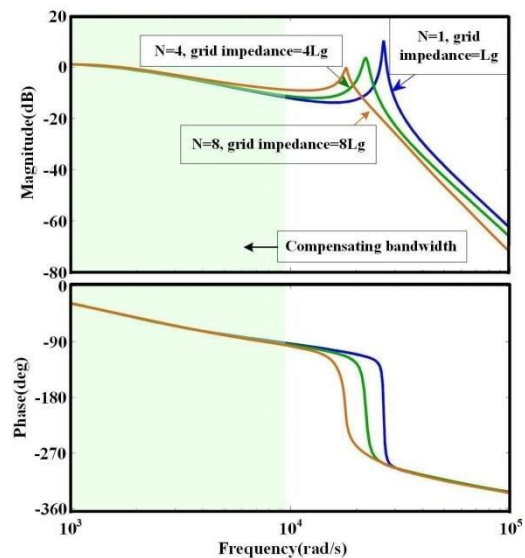


Fig. 7. Bode diagram of $I_g(s)/I_{ref}(s)$ with different grid impedance

sine wave part. For the traditional secluded SAPF, as the recurrence of thunderous pinnacle diminishes while the quantity of modules N builds, the recurrence band of remunerating current will come near the full pinnacle. The steadiness edge likewise drops and reverberation will in general happen. Besides, it can likewise be seen from Fig.7 that the control transmission capacity is never again adequate for high request music remuneration for an expanded N . At long last, in the customary particular SAPF with a similar channel inductance and control parameters, a tradeoff between the dynamic reaction and the steadiness control is hard to get either by aloof segments plan or by dynamic damping control. This is the test that the present exertion plans to in a general sense address.

III. Lcl Filter Design, Resonance Analysis And Self-Adaptive Active Damping For Hybrid Modular Three-Level Sapf

In light of the summed up displaying of secluded SAPF and comprehension of their impediments, a novel cross breed particular three-level SAPF is proposed in this paper. The half and half framework consolidates bigger limit modules and littler modules. Bigger limit modules have higher LCL channel esteems and lower exchanging recurrence while littler limit modules have lower LCL channel esteems and higher exchanging recurrence. The plan intends to remunerate the lower request sounds and higher request music separately. In the proposed crossover framework, the traditional SAPF remunerating band as appeared in Fig.7 is separated into high and low request groups. Such a structure utilizing diverse LCL channel parameters for two remunerating groups enables more space to accomplish tradeoff between the dynamic reaction and the framework soundness control. Next amodular SAPF

LCL channel plan technique and a secluded framework reverberation examination will be exhibited, trailed by a novel selfadaptive dynamic damping procedure for crossover measured SAPF.

A. LCL design of modular SAPF

Given the particular SAPF capacities and confinements uncovered in area II, a plan technique for the SAPF latent channel must be created. A well ordered methodology to plan the LCL channel for a particular SAPF is proposed as pursues:

- First the inverter side inductance $L1$ is planned so as to restrict the present swell created by the SAPF inside 10% evaluated remunerating current [26], [27];
- The worthy degree of the responsive capacity to be consumed by the channel capacitor under evaluated conditions is chosen, and this decides the capacitor esteem [26];
- The by and large inductance of inductors introduced ought to be constrained to well beneath the 10% of the base impedance;
- As appeared from the demonstrating investigation in area II, the identical matrix side inductance changes with the parallel number of modules;
- Minimize the channel volume by utilizing lower inductances and higher capacitances. This is because of the way that SAPF repaying current causes higher voltage drop than the framework tied inverter;
- The reverberation point ought to be higher than that for the sine wave lattice tied inverters in light of the fact that SAPF's repaying band is more extensive;
- Last the present variety rate produced by the SAPF ought to be more prominent than the normal current. This can be communicated by:

$$L < \frac{U_{dc} - 1.1U_g}{I_c} \quad (11)$$

where U_{dc} and I_c are the SAPF dc connect voltage and remunerating current, separately, which forces another restriction to the converter side inductance

B. Resonance and stability analysis of hybrid modular three level SAPF

To research the following and reverberation issues among modules of various limits, rearranged comparable circuit models can be gotten from Fig.5. Fig.8(a) demonstrates a streamlined model for the bigger SAPF module #1 and Fig.8(c) indicates rearranged model for the littler SAPF module #2. In Fig.8(a) and (c), X speaks to the quantity of bigger limit modules and Y speaks to the quantity of littler limit modules. The #1 and #2 converters represent one bigger and one littler limit modules, separately. The other (X - 1) bigger limit modules and (Y - 1) littler limit modules can be disentangled as impedances. In view of this disentanglement, we can get the bode graph of $I_g L(s)/I_{ref} L(s)$ appeared in Fig.8(b), where (X - 1) bigger limit module impedance, Y littler limit module impedance and framework impedance are plotted. The repaying current of #1 SAPF with a data transmission running from 150Hz to 650Hz, is separated by the impedance of the network, (X-1) SAPF with bigger limit and Y SAPF with lower limit. It tends to be seen that inside the repaying band under thirteenth request, matrix impedance is a lot littler than the impedance of (X - 1) SAPF and Y SAPF. The remunerating current is chiefly infused into the network. It is unmistakably demonstrated that the repaying current band of SAPF #1 is a long way from the reverberation top and gives adequate control

transmission capacity. In this manner, it enables more space to tradeoff between the remunerating dynamic reaction and steadiness control.

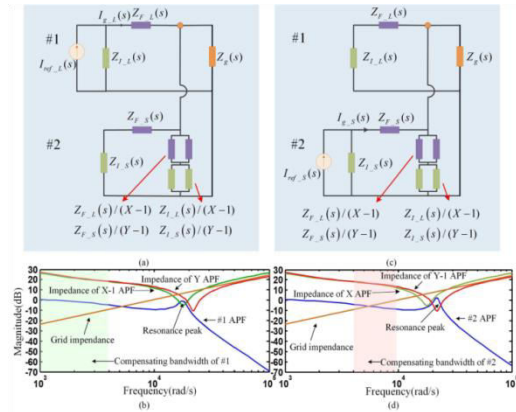


Fig. 8. Equivalent circuit and bode diagram of the hybrid parallel SAPF

For SAPF #2, the littler limit module infuses remunerating sounds higher than the thirteenth request, i.e., from 650Hz onwards. As appeared in Fig.8(d), the Bode outline of $I_g S(s)/I_{ref} S(s)$ demonstrates that littler LCL parameters configuration push the resounding pinnacle higher and makes adequate control transmission capacity for high request remunerating current. As opposed to the regular particular SAPF in Fig.7, Fig.8(d) demonstrates that the secluded SAPF empowers more prominent edge and data transmission to tradeoff between powerful reaction and solidness control. In addition, the higher exchanging recurrence and low inductance further improve the present following reaction capacity. As indicated by the repaying band for SAPF #2, the framework impedance is moderately enormous, yet X SAPF is structured with higher LCL parameters. Accordingly, lattice impedance is still a lot littler than the impedance of X SAPF. Further, the higher request consonant parts are normally littler in extent, and thus, less lower limit modules, conceivably a couple, is required. In short it tends to be inferred that the repaying current essentially streams

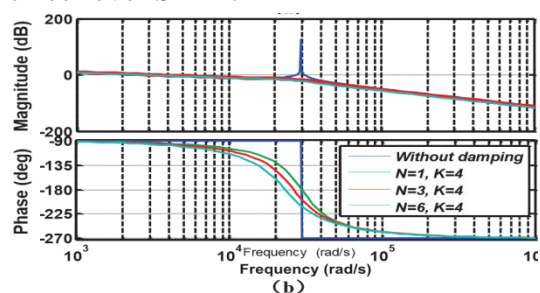
into the grid. It ought to be noticed that in the half breed framework proposed in this paper, the dynamic reaction and the security control are adjusted by latent channel configuration as well as constrained by dynamic damping. Along these lines, the reverberation shouldn't be smothered further by the controller increase guideline as that in [14], [15] which bargain current following exactness.

In this paper, to accomplish quick current unique reaction and remarkable steadiness control, a novel self-versatile reverberation smothering procedure is then proposed for the half breed paralleled framework.

C. Limitations analysis of conventional resonance damping methods and the novel self-adaptive active damping for hybrid modular three-level SAPF

In spite of the fact that LCL channels can more readily fulfill matrix interconnection guidelines with fundamentally littler size and cost, they additionally trigger reverberation between the inverter and the lattice. A functioning or a detached damping measure is typically embraced to smother potential resonances. If there should be an occurrence of secluded SAPFs, a functioning damping strategy creates better results. The dynamic damping technique proposed in [27] is generally utilized in the network tied inverter, which presents the capacitor branch present as the input amount to improve the damping impact of the framework. Be that as it may, in the strategy portrayed in [27], the damping input control coefficient K is fixed ignoring the lattice side impedance, and the converter side inductance may fluctuate. Consider the model where the converter side inductance differs, if K is constantly fixed when the inductance brings due down to the adjustment in burden current, the framework steadiness edge contracts as appeared in

Fig.9(a). As appeared in Fig.9(b), with an expanded number of modules N in parallel, lattice impedance develops to $N \cdot L_g$. The resounding recurrence of the SAPF framework shifts towards the left and the solidness edge of the SAPF framework decreases. As appeared from the measured SAPF displaying, the equal network impedance differs generally because of the quantity of modules associated. Besides, the converter side inductance likewise changes significantly because of the high peak factor of repaying current as opposed to customary sine wave inverter. Hence, the strategy in [27] can't be legitimately utilized. Rather, we propose a novel self-versatile dynamic damping for the cross breed SAPF. In this technique, K isn't fixed yet got through enhancement on the modules number, and all the more significantly, the moment inductance dictated by the remunerating current. The epic self-versatile dynamic damping strategy dependent on capacitor branch current criticism for the crossover particular three level SAPF is appeared in Fig.10. The new technique includes a variable dynamic damping coefficient K_0 for various estimations of N and various benefits of remunerating current. Its comparing control outline is appeared in Fig.11. In this paper, just the inductor current following reference is examined, $E(s)$ speaking to the lattice voltage carries on as an unsettling influence and is viewed as zero when investigating the reverberation and soundness of half and half secluded three-level SAPF.



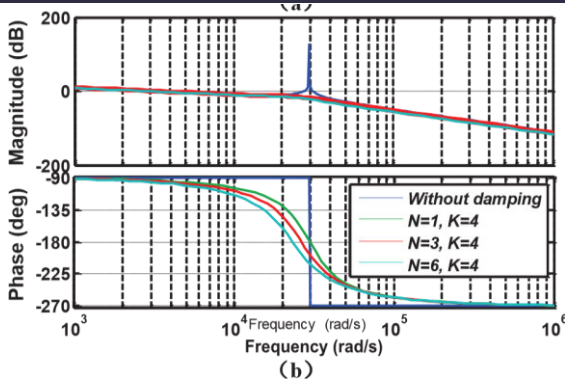


Fig.9.(a)Frequency characteristics with different output current (b)Frequency characteristics with different number of parallel units

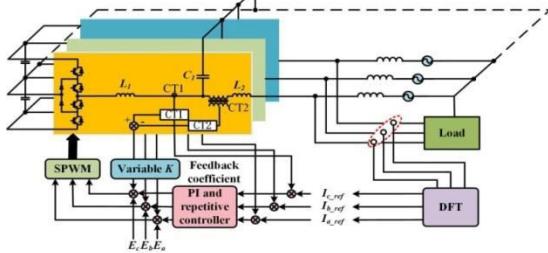


Fig. 10. Controller design with proposed self-adaptive active damping

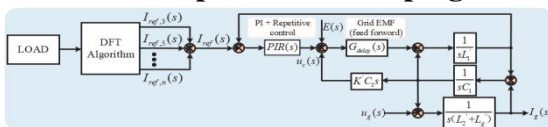


Fig. 11. Novel self-adaptive active damping strategy

In this manner ignoring $E(s)$ and the impact of $G_{delay}(s)$, the open circle move capacity of the framework can be given by.

$$G_{gc}(s) = \frac{I_g(s)}{u_c(s)} = \frac{1}{L'_1(L'_2 + L'_g)C_1 s^3 + K'(L'_2 + L'_g)C_1 s^2 + (L'_1 + L'_2 + L'_g)s} \quad (12)$$

where K_0 is the variable criticism coefficient, are the genuine inductances as an element of the yield current and L_0 is the comparable matrix impedance of one SAPF in the half breed parallel SAPF, and can be determined by the cross breed identical circuit in Fig.8.

To improve the dialog, $G_{gc}(s)$ can be re-composed as the result of an essential circle and a second order request wavering circle:

$$G_{gc}(s) = \frac{1}{L'_1(L'_2 + L'_g)C_1 s^2 + K's/L'_1 + \omega_{res}^2} \quad (13)$$

where ω_{res} is the resonance frequency of the second order oscillation loop.

$$\omega_{res}^2 = \frac{L'_1 + L'_2 + L'_g}{L'_1(L'_2 + L'_g)C_1} \quad (14)$$

According to the definition of damping ratio ξ in the second order oscillation loop, it can be given as:

$$\xi = \frac{K'}{2L'_1\omega_{res}} \quad (15)$$

In the under damped second order oscillation loop, given a decrease in ξ , the overshoot increases and the response time decreases. On the other side, with the increase of ξ , the overshoot decreases, but the system response slows down. According to the control theory, when damping ratio equals to 0.707, the system overshoot is moderate and the regulation time is short, where the system is at the best damping condition. In SAPF applications, at the point of $\xi = 0.707$, the hybrid SAPF system can reach an optimal tradeoff between resonance suppression and time response. Therefore, the optimum damping ratio of the second order oscillation loop is chosen as $\xi = 0.707$.

Take $\xi = 0.707$ and substitute Eq.(14) into Eq.(15), we can attain the expression of the optimized feedback coefficient K^0 .

$$K^0 = \sqrt{\frac{2L'_1(L'_1 + L'_2 + L'_g)}{(L'_2 + L'_g)C_1}} \quad (16)$$

Further examination of Fig.11 demonstrates that the framework solidness is essentially controlled by the criticism coefficient K_0 . Fig.12 demonstrates summed up root locus of (12) with various K_0 . The steady scope of K_0 is from 0.714 to 11. In this way, in our framework, to guarantee K_0 determined by (16) is in a sensible range, we oblige the criticism coefficient K_0 as follows:

$$K^0 = \begin{cases} 0.714 & K' < 0.714 \\ \sqrt{\frac{2L'_1(L'_1 + L'_2 + L'_g)}{(L'_2 + L'_g)C_1}} & 0.714 < K' < 11 \\ 11 & 11 < K' \end{cases} \quad (17)$$

The proposed novel self-versatile dynamic damping control technique for the half and half secluded three level SAPF can be utilized

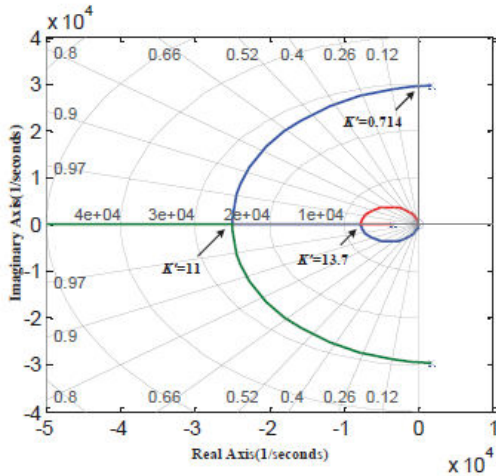


Fig. 12. The generalized root locus of (12) with different K^0

not just in mechanical applications where variable burdens are associated with the framework, yet in addition, the situations where there is communication of various SAPF frameworks associated with a frail power matrix, and an expanded steadiness edge is required for the security of SAPF framework.

IV. SIMULATION AND EXPERIMENTAL RESULTS

A. Simulation results

Impact of the inductance and the adjustment in the module number on the framework soundness edge is delineated in Fig. 9 with a consistent damping input coefficient K . So as to decipher it unequivocally, we do two reproductions in MATLAB/Simulink. Fig. 13 demonstrates the reenactment results for three SAPFs in parallel activity with the heap current significantly increased at $t = 0.16s$. The channel inductance is balanced by the difference in the yield current at $t = 0.16s$, while the input coefficient K of dynamic damping is kept steady. We can see from the outcomes that before $t = 0.16s$, the half and half SAPF framework with two

bigger units and one little unit repays the sounds well. The heap current and yield flows significantly increased at $t = 0.16s$, and thusly the inductance diminishes. Be that as it may, because of the unaltered criticism coefficient K , reverberation happens in the framework. This is as per the decline in dependability edge in Fig. 9(a).

In Fig. 14, the working condition is equivalent to depicted in Fig. 13 before $t = 0.16s$ with the exception of that the inductance is set as a steady worth. After $t = 0.16s$, load current duplicates and we turn on another three SAPF units, which implies that the parallel unit number N increments from 3 to 6. Framework reverberation happens comparably on account of the unaltered K . The recreation results again coordinate the ends got from Fig. 9(b).

B. Experimental results

The crossover SAPF framework as appeared in Fig. 15 is likewise actualized to confirm the proposed plan and resonance suppression system.

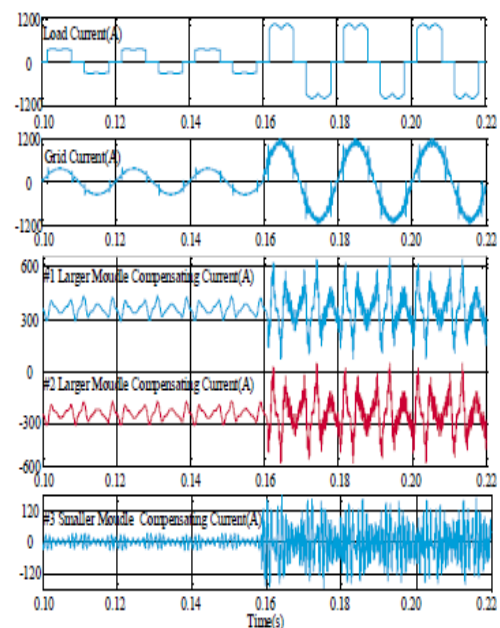


Fig. 13. Simulation results of output current increase with three SAPF in parallel operation

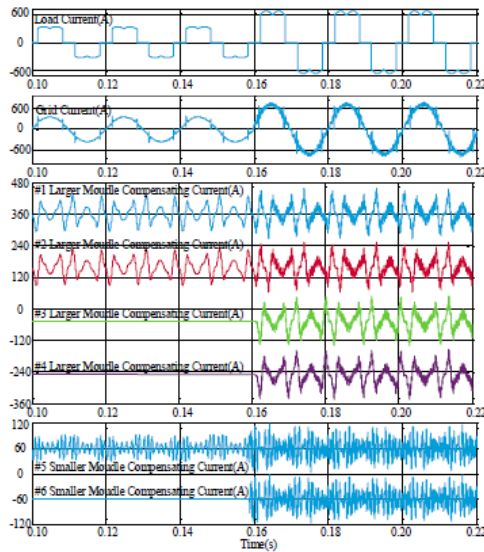


Fig. 14. Simulation results of parallel units increase with six SAPF in parallel operation

The bigger module power ratings is fixed at 100A intending to remunerate the low request sounds under thirteenth request, and the littler 50A module repaying the high request music higher than thirteenth request. The fundamental parameters are recorded in Tab. I.

The principle circuits are appeared in Fig.16. 100 An Infineon three level power module F3L100R07W is picked for 50A littler module. Two F3L100R07W are associated in parallel to fill in as the 100 A bigger power module as appeared in Fig.16(b).

Fig.17&Fig.18 demonstrate the self-versatile damping test



Fig. 15. Hybrid modular three-level SAPF prototype

TABLE I
PROTOTYPE AND THE EXPERIMENTAL PARAMETERS

Item	Value
Grid frequency	50Hz
Switching frequency(100A,50A)	20kHz, 40kHz
Phase voltage(RMS)	230V
DC voltage	800V
100A module LCL	800/4μH, 20μF, 75μH
50A module LCL	200/2μH, 10μF, 50μH
IGBT module	F3L100R07W2E3

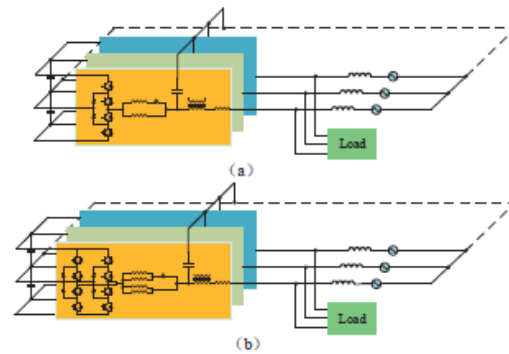


Fig. 16. (a) 50A module topology (b) 100A module topology

Results. In Fig.17, Channel 1 and 5 are burden current and lattice current, individually. Before $t = 32ms$, #2 SAPF (100A) and #3 SAPF (50A) are in stable activity utilizing conventional dynamic damping technique as appeared by Channel 2, 3 and 4. At $t = 32ms$, #1 SAPF (100A) begins its activity as appeared by Channel 2 utilizing customary dynamic damping strategy. It tends to be seen from the waveforms that the conventional dynamic damping strategy with a fixed damping criticism coefficient neglects to viably stifle reverberation on the grounds that the quantity of parallel modules N changes. After $t = 64ms$, the measured framework begins to work with the proposed self-versatile dynamic damping strategy, and the reverberation is all around stifled. Fig.18 demonstrates the test results with an adjustment in burden current. Channel 2, 3 and 4 demonstrate the remunerating flows of #1 SAPF(100A), #2 SAPF(100A), #3 SAPF(50A), which are steady before $t = 32ms$ using conventional dynamic damping. Nonetheless, with burden

multiplied at $t = 32\text{ms}$, reverberation begins to show up in measured framework. At $t = 64\text{ms}$, the proposed selfadaptive dynamic damping is connected to the framework and reverberation vanishes. This is on the grounds that the criticism coefficient presently differs with change in burden current. Subsequently, the reverberation stifled, rendering the framework stable.

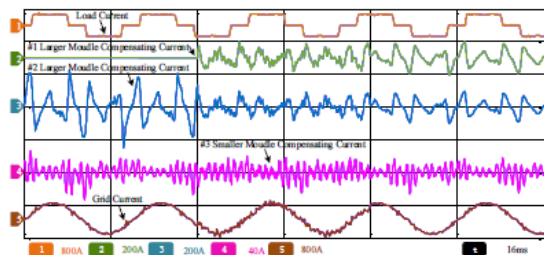


Fig. 17. Compensating current of hybrid modules with different damping methods

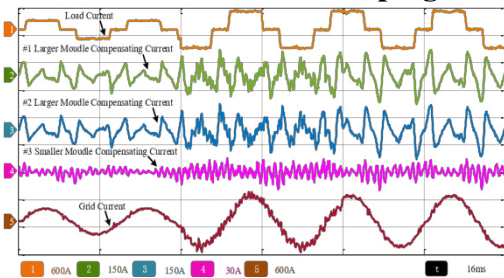


Fig. 18. Compensating current of hybrid modules with load change

It very well may be finished up from Fig.17 and Fig.18 that with a fixed input coefficient K , reverberation happens when inductance or parallel number N change. These trial results are steady with the examination in Fig.9 and the recreation results in Fig.13 and Fig.14. Fig.19 demonstrates the remunerating flows of 50A module and 100A modules in parallel utilizing the self-versatile damping procedure together with the range of network current when pay. From Channel 1 to Channel 5 are: i) the heap current; ii) modules #1 and #2 (100A) repaying current; iii) module #3 (50A) remunerating current, and iv) the network current after pay. This outcome demonstrates that the 50A module

has quick powerful reaction since it has lower LCL parameters and higher exchanging recurrence. The THD of matrix current is 27.13% before the remuneration and 4.89% after.

V. CONCLUSION

This paper enhances customary particular SAPF numerical model to research tradeoffs between unique reaction and dependability control. As indicated by the investigation results got from the model, a novel half breed secluded three-level SAPF structure is proposed. Rather than past techniques, the proposed framework is made out of two modules, each with various current conveying limits, LCL channel parameters and exchanging frequencies. At last, a novel self-versatile reverberation concealment procedure is proposed to consider the varieties in the quantity of modules and burden current.

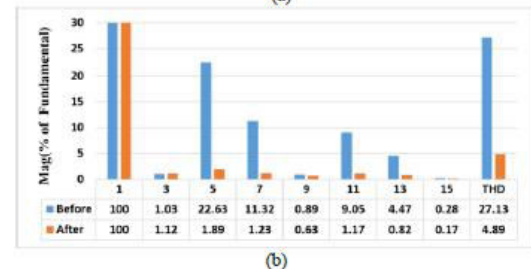
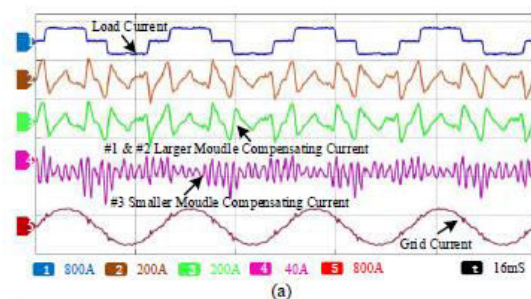


Fig. 19. (a) Experimental results of three SAPF in parallel (b) THD of grid current

Hypothetical examination and exploratory outcomes affirm that the half breed particular SAPF and its self-versatile reverberation concealment procedure can accomplish a superior tradeoff between unique reaction and security control as contrasted and the regular measured SAPF.

The proposed framework might be utilized in modern applications, specifically for power quality improvement in feeble power matrices.

REFERENCES

1. J.Tooth, G.Xiao, X.Yang, and Y.Tang, "Parameter plan of a novel arrangement parallel-thunderous lcl channel for single-stage half-connect dynamic power channels," *IEEE Transactions on Power Electronics*, vol. 32, no. 1, pp. 200–217, Jan 2017.
2. J.C.Alfonso-Gil, E.Perez, C.Arino, H. Beltran, "Advancement' calculation for particular remuneration in a shunt dynamic power channel," *IEEE Transactions on Industrial Electronics*, vol. 62, no. 6, pp. 3351–3361, 2015.
3. M.Angulo, D.A.Ruiz-Caballero, J.Lago, M.L.Heldwein, and S.A.Mussa, "Dynamic power channel control system with understood shut circle current control and thunderous controller," *IEEE Transactions on Industrial Electronics*, vol. 60, no. 7, pp. 2721–2730, 2013.
4. J.He, Y.W.Li and F.Blaabjerg, "Adaptable microgrid control quality upgrade utilizing versatile mixture voltage and current controller," *IEEE Transactions on Industrial Electronics*, vol. 61, no. 6, pp. 2784–2794, 2014.
5. P.Acuna, L.Moran, M.Rivera, J.Dixon, and J.Rodriguez, "Improved' dynamic power channel execution for inexhaustible power age frameworks," *IEEE exchanges on power gadgets*, vol. 29, no. 2, pp. 687–694, 2014.
6. H.Yi, F.Zhuo, Y.Zhang, Y.Li, W.Zhan, W.Chen, J.Liu, "A source-current-recognized shunt dynamic power channel control plan dependent on vector resounding controller," *IEEE Transactions on Industry Applications*, vol. 50, no. 3, pp. 1953–1965, 2014.
7. R.Dian, W.Xu, and C.Mu, "Improved negative grouping current identification and control procedure for h-connect three-level dynamic power channel," *IEEE Transactions on Applied Superconductivity*, vol. 26, no. 7, pp. 1–5, 2016.
8. S.Rahmani, N.Mendalek, and K.Al-Haddad, "Exploratory structure of a nonlinear control strategy for three-stage shunt dynamic power channel," *IEEE Transactions on Industrial Electronics*, vol. 57, no. 10, pp. 3364–3375, 2010.
9. Z.Wang, C.Xie, C.He, G.Chen, "A waveform control procedure for high power shunt dynamic power channel dependent on redundant control calculation," in *Applied Power Electronics Conference and Exposition (APEC), 2010 TwentyFifth Annual IEEE*. IEEE, 2010, pp. 361–366.
10. Y.Tang, P.C.Loh, P.Wang, F.H.Choo, F.Gao, F.Blaabjerg, "Summed up structure of elite shunt dynamic power channel with yield lcl channel," *IEEE Transactions on Industrial Electronics*, vol. 59, no. 3, pp. 1443–1452, 2012.